

Theoretical Study of Hydrogen Chemisorption to Nitrogen-Substituted Graphene-Like Compounds

Megumi Kayanuma,*,† Tamio Ikeshoji,†† and Hiroshi Ogawa

Research Institute for Computational Sciences, National Institute of Advanced Industrial Science and Technology, Chuo-2, 1-1-1 Umezono, Tsukuba, Ibaraki 305-8568

Received April 16, 2010; E-mail: kayanuma@unistra.fr

Interaction between nitrogen-substituted graphene-like compounds and hydrogen was investigated using ab initio molecular orbital methods to assess hydrogen storage. We adopted coronene as a model molecule for fragmented graphene-like carbon materials and compared the chemisorption energies of hydrogen on pure and N-substituted coronens by changing nitrogen positions. Among the assumed 19 N-substituted models with different substitution sites, three representative models were selected and closely examined to reveal the dependences on both nitrogen-substitution and hydrogen-adsorption positions. Optimized structures of the chemisorbed products are largely stabilized by N-substitution at a certain position. Positive or negative energy gain was apparent depending on both substituted sites of N and adsorbing position of H_2. The results suggest that it is possible to improve hydrogen storage properties of graphene-like materials by N-substitution.

Hydrogen has attracted much attention as a clean and renewable fuel in recent years. To establish hydrogen-based energy systems, considerable advancement in technologies for economical production and storage of hydrogen are required especially for mobile applications.[1–5] Hydrogen storage in solid-state systems is simpler and safer than storage as either compressed or liquid hydrogen. Therefore, various hydrogen storage materials based on metal hydrides, chemical hydrides, and hydrogen absorption materials have been studied widely.

Lightweight carbon material is a candidate for use as a hydrogen storage material for mobile applications. Hydrogen interacts with carbon materials through physisorption and chemisorption.[6–10] Physisorption, resulting from van der Waals attractive forces, has binding energy of 4–5 kJ mol^{-1}. Chemisorption originates from covalent C–H interaction; its binding energy is more than 100 kJ mol^{-1}. For reversible hydrogen absorbtion/desorbtion in the temperature range of -20 to 50 °C and at moderate pressures, the ideal hydrogen binding energy is estimated to be 20–40 kJ mol^{-1}.[6] Consequently, physisorption is too weak but chemisorption is too strong. Methods to improve hydrogen storage properties have been studied: changing structures, adding heteroatoms, and catalyzing the dissociation of hydrogen molecules to hydrogen atoms.

Recently, carbon materials with large surface area have attracted attention. Among the carbon materials including carbon nanotubes (CNT), carbon nanohorns, and fullerenes, microporous carbons offer many beneficial features, i.e., high surface area, high pore volume, low weight, and tunable pore structures.[11] Various microporous carbons have been synthesized using different templates and carbon precursors.[12–17] Above all, microporous carbon synthesized by Kyotani et al.[12] has very high surface area with uniform micropores. Based on results of experimental analyses, they proposed a crude model of the microporous carbon consisting of single, curved, nonstacked, and nanometer-sized graphene fragments with numerous edges.[17]

On the other hand, growing interest has surrounded nitrogen-substituted and boron-substituted carbon materials because of their unique electronic, mechanical, optical, and adsorption properties.[18] For example, nitrogen-doped carbon-based nanomaterials are anticipated for use in catalyzing oxygen reduction reactions.[19,20] In the area of hydrogen storage, Viswanathan et al.[21] synthesized CNTs containing nitrogen or boron and reported that the amount of hydrogen uptake is enhanced by substitution. They demonstrated that the dissociation energy of hydrogen molecule decreases in the presence of substituted CNT using density functional theory (DFT) calculations. Zhou et al. calculated hydrogen molecular and atomic adsorption energy of B-doped or N-doped CNT using DFT. They showed that both B-doping and N-doping decreased the hydrogen molecular adsorption energies (i.e., diminish physisorption) but that N-doping decreased hydrogen atomic adsorption energy (i.e., benefit for releasing of atomic hydrogen adsorbed onto CNTs).[22] As for N-substitution in porous carbon, both positive[23,24] and negative[25] effects are experimentally reported. Wang et al. reported that B-doping and N-doping cause a positive effect for hydrogen storage.[18] In contrast, Nishihara et al. reported that N-doping did not affect the hydrogen uptake.[12] Such variation of doping effects have not been investigated.

† Present address: Institut de Chimie, UMR 7177 CNRS/ Université de Strasbourg, 4 rue Blaise Pascal 67000 Strasbourg, France

†† Present address: New Industry Creation Hatchery Center, Tohoku University, 6-6-10 Aoba, Aramaki, Aoba-ku, Sendai 980-8579

Published on the web January 1, 2011; doi:10.1246/bcsj.20100111

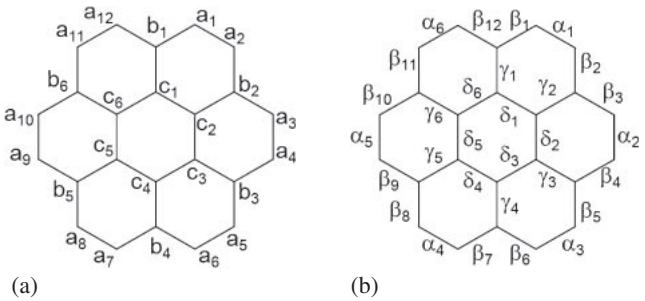

Figure 1. Notation of atomic sites (a) and bonds (b) in coronene ([6]circulene) used for this study.

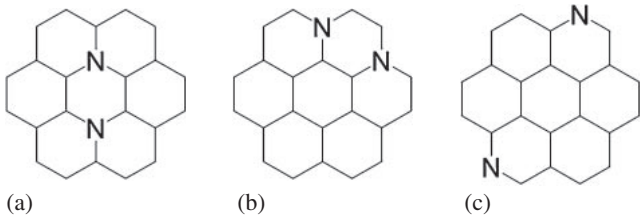

Figure 2. Three typical N-substituted model molecules; "N-I" (a), "N-II" (b), and "N-III" (c).

Although nondissociative physical adsorption has been considered to be a dominant mechanism for hydrogen storage in graphene-like materials,[10] the importance of chemisorption has also been pointed out by many authors,[26–30] especially, on the "hydrogen spillover" phenomenon.[31] The aim of this study is to reveal how the nature of hydrogen adsorption on a small fragment of graphene sheet and how nitrogen substitution on such materials affects hydrogen chemisorption. Ab initio molecular orbital study is used to evaluate the hydrogen chemisorption energies on some nitrogen-substituted model molecules for the fragmented graphene-like compounds.

Computational Method

For a simple and small model representing a nanometer-sized graphene fragment in carbon-based hydrogen storage materials, such as microporous carbon, we assume coronene ([6]circulene, Figure 1) as the fundamental molecule. Though microporous carbon is expected to consist of various graphene fragments with different sizes, here we selected one of the simplest model molecules, of which size is comparable to a unit of microporous carbon ($C_{36}H_9$) synthesized by Kyotani et al.[17] For simplicity, we only consider flat carbon surfaces in this study, and the effect of curvature for pure carbon surface is discussed elsewhere.[32] The main aim of this study is to clarify the effects of nitrogen-substitution at not only graphene-like regions but also edge sites because microporous carbon contains abundant edge carbon atoms[17] and we expected these edge sites are very important in such systems. The simple and symmetric structure of coronene is effective for this purpose. In addition, it has been suggested that coronene is also a good model for graphite surface.[33,34] They showed that the calculated binding strength and normal vibrational frequency of atomic H on coronene were very close to the experimental values on highly ordered pyrolytic graphite.[34]

We examined various patterns of N-substitution in coronene. Zhu et al. showed that substitutions of two boron atoms provide consistent and reliable results, but substitutions of only one boron atom result in contradictory conclusions.[35] Therefore, we examined cases, in which two carbon atoms at various positions are replaced with nitrogen atoms, and discussed the dependency of interaction energies on the substitution sites. Such site dependency has not been discussed previously. These models are distinguished by the combination of substitution sites. In this paper, the numbering of carbon atoms in coronene is defined with respect to the edge (a_1–a_{12}), middle (b_1–b_6), and inner (c_1–c_6) carbon atoms, as presented in Figure 1a. Coronene has C–C bonds of four types, which we designate from outside as α (α_1–α_6), β (β_1–β_{12}), γ (γ_1–γ_6), and δ (δ_1–δ_6) (Figure 1b).

To consider weak chemisorption of hydrogen on the graphene fragment, MP2 method which considers electron correlation is used to qualitatively evaluate how the interaction energy with two H atoms (dissociated H_2 molecule) varies by nitrogen substitution sites. Geometry optimizations of pure and N-substituted coronenes were done at HF level of ab initio molecular orbital theory with 6-31G(d) basis set. GAMESS program package[36] was used in the whole calculations. We first examined the case of N-substitution for C at middle and inner positions (b_1–b_6 and c_1–c_6). We also examined the models with N-substitution at the edge positions (a_1–a_{12}), in which two C–H groups are replaced with nitrogen atoms. The HOMO–LUMO gaps of these compounds were evaluated as a reference for reactivity with hydrogen.

To gain information necessary to support a detailed discussion, we selected three typical model compounds: "N-I," which has the smallest HOMO–LUMO gap (Figure 2a); "N-II," which is the most stable among those having nitrogen at a non-edge position (Figure 2b); and "N-III," which has edge position nitrogen atoms (Figure 2c). The stabilities of H_2 dissociative adsorption products on pure and these three N-substituted coronenes were estimated at MP2/6-311G(d,p)//HF/6-31G(d,p) level of theory.

Results and Discussion

Stability and Reactivity of N-Substituted Compounds. Table 1 presents HOMO and LUMO energies of coronene and 19 N-substituted coronenes calculated at HF/6-31G(d) level of theory. The variation is apparently classified by the combination of the substitution sites: edge (a_i), middle (b_i), and inner (c_i). In cases of non-edge (inner and/or middle site) substitution, the systems have two additional electrons compared with the pure carbon case and their HOMO corresponds to LUMO of coronene. In these cases, HOMO–LUMO gaps are smaller than that of pure carbon (864 kJ mol^{-1}) and vary with the position of nitrogen from 791 kJ mol^{-1} for b_1–c_1 substitution to 357 kJ mol^{-1} for c_1–c_4 substitution. In the case of edge substitution (a_i–a_j), on the other hand, the HOMO–LUMO gaps vary between 835 to 858 kJ mol^{-1} and are almost identical with that of coronene. The systems in this case have the same number of electrons and almost the same electronic structure as the pure coronene. The total energies of the N-substituted coronenes were also examined for non-edge and edge substitution cases. The most stable structures are obtained, respectively, by b_1–b_2 and a_1–a_5 substitution. The relative

Table 1. Energies (in kJ mol^{-1}) of HOMO, LUMO, HOMO–LUMO Gap (*H–L*), and Relative Energy (ΔE)[a] of Pure Coronene (C) and All Possible 19 N-Substituted Coronenes[b] Having Closed Shell Structure Calculated at HF/6-31G(d) Level

	HOMO	LUMO	*H–L*	ΔE
C	−675.8	188.5	864.3	—
(a)				
a_1–a_2	−727.5	124.7	852.2	110.6
a_1–a_3	−719.4	136.8	856.2	4.9
a_1–a_4	−718.9	136.5	855.4	2.2
a_1–a_5	−719.1	138.9	858.0	0
a_1–a_6	−707.6	128.1	835.7	4.1
a_1–a_7	−708.4	132.3	840.7	0.3
a_1–a_8	−717.8	139.4	857.2	0.6
a_1–a_{10}	−719.1	136.0	855.1	2.0
a_1–a_{12}	−709.1	131.5	840.7	6.6
(b)				
b_1–b_2	−474.2	201.4	675.5	0
b_1–b_3	−371.2	159.6	530.9	126.6
b_1–b_4	−445.0	251.3	696.3	8.5
b_1–c_1	−562.1	228.4	790.5	86.6
b_1–c_2	−404.9	165.7	570.5	127.4
b_1–c_3	−446.1	219.0	665.0	60.6
b_1–c_4	−374.7	168.6	543.2	131.3
c_1–c_2	−533.5	207.2	740.7	152.9
c_1–c_3	−397.0	176.4	573.4	162.8
c_1–c_4	−311.9	44.9	356.8	288.8

a) The values of ΔE are given as the relative ones to the most stable compound in each series (a) and (b): a_1–a_5 for edge substitution coronenes (a) and b_1–b_2 for non-edge substitution coronenes (b). b) Positions of nitrogen atoms (a_1 to c_4) are denoted in Figure 1a.

energies of N-substituted coronenes measured from the most stable cases are also presented in Table 1. Among non-edge substituted coronene, the energetically most unstable isomer is the compound of c_1–c_4 substitution, of which the energy is 289 kJ mol^{-1} higher than that of the most stable one, b_1–b_2 substitution. In contrast, edge substituted coronenes have almost identical energy (≈6.6 kJ mol^{-1}), except for a_1–a_2 (110.6 kJ mol^{-1}) in which two nitrogen atoms are located next to each other. These results suggest that the properties of N-substituted coronenes change greatly and vary widely depending on the nitrogen position in the case of non-edge substitution. Meanwhile, the reactivity is expected to be comparable among edge-substituted cases and to be similar to that of pure coronene when we estimated the reactivity from the HOMO–LUMO gaps.

For detailed analysis in the following sections, we selected three typical N-substituted coronenes. First is that obtained by substitution at c_1–c_4 (we call it "N-I"), which has the smallest HOMO–LUMO gap (356.8 kJ mol^{-1}) and which is expected to have high reactivity. Second is by the substitution at b_1–b_2 ("N-II"), which is the most stable isomer among models with non-edge substitution. We select a third model molecule, a_1–a_8 substitution ("N-III"), from among those of edge substitution.

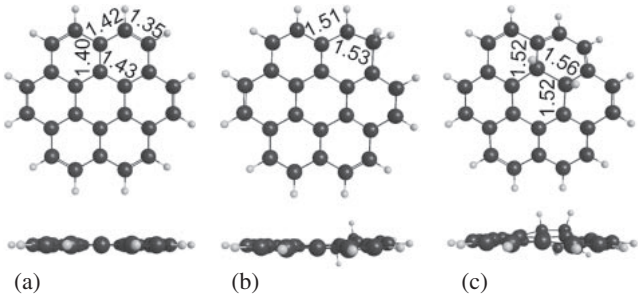

Figure 3. Optimized structures of H_2 dissociative adsorption products on α (b) and δ (c) site in comparison with that of pure coronene (a). Values in the figure are C–C bond lengths in Å.

N-III has C_{2v} symmetry and its HOMO–LUMO gap almost matches that of pure coronene (smaller by only 7 kJ mol^{-1}).

Stability of the Products of H_2 Dissociative Chemisorption. Geometry optimizations of the products of H_2 dissociative adsorption on pure and N-substituted coronenes have been conducted at HF/6-31G(d,p) level and their energies were calculated at MP2/6-311G(d,p) level. Figure 3 shows the variation of optimized structures of pure coronene (a) and chemisorbed products with two additional hydrogen atoms on C–C bond at α site (b) and δ sites (c). By addition of hydrogen, positions of carbon atoms deviate from the plane and related C–C bonds lengthen by 0.1–0.2 Å. This means that the nature of these C–C bonds changes from sp^2 bonding to sp^3 like bonding. It is noteworthy that the H atoms on α site locate on both sides of the coronene plane.

Table 2 presents a summary of adsorption (chemisorption) energies (E_{ad}) for all independent chemisorption sites in pure and three N-substituted models. The adsorption energies were determined as the difference between the energies of chemisorbed product and the reference state (the corresponding model compound and H_2 molecule at their equilibrium structures) for pure and N-substituted models. In the pure coronene case, the chemisorbed product on-edge C–C bond (α site) is more stable than the reference state by 51.3 kJ mol^{-1}. Formation of C–H bonds on other sites (β, γ, and δ) engenders large negative values of E_{ad}, which means that hydrogen chemisorption on non-edge sites destabilizes the system. These results suggest that hydrogen chemisorption can occur only on edge bonds. For model N-I, adsorption energies are higher than that of pure coronene for all chemisorption sites. Chemisorbed products are more stable than the reference states, except for β_3, γ_1, γ_2, and δ_1. In the case of γ_1 and δ_1, one of the added H atoms bonds to a nitrogen atom (E_{ad} is −128.0 and −157.0 kJ mol^{-1} for γ_1 and δ_1, respectively). This suggests that N-substitution at this site stabilizes the chemisorbed products of H_2. In the case of N-II, stability of the products varies with the chemisorbed site where two additional C–H bonds are formed. Chemisorbed products at α_3, β_1, β_7, γ_1, and γ_4 are less stable than those of pure coronene. As with the pure carbon cases, chemisorption at most of the inner sites (β, γ, and δ) destabilizes the system, except for δ_1. In particular, formation of N–H bonds notably seems to destabilize the system (E_{ad} is −128.4 and −234.0 kJ mol^{-1} for β_1 and γ_1). Among the chemisorbed products at the edge sites, the α_3 case is less stable

Table 2. Adsorption (Chemisorption) Energies[a] of H_2, E_{ad} (kJ mol^{-1}) = {E(Pure/N-Substituted Coronene) + $E(H_2)$} − E(Product), for Pure and Representative N-Substituted Coronenes with Independent Chemisorption Sites of Target Bond (α_n, β_n, γ_n, and δ_n)[b] Calculated at MP2/6-311G(d,p)//HF/6-31G(d,p) Level

	n	α_n	β_n	γ_n	δ_n
Pure	—	+51.3	−116.1	−151.6	−207.3
N-I	1	+83.4	+63.4	−128.0	−157.0
	2	+79.5	+46.9	−59.1	+33.9
	3		−92.2		
N-II	1	+162.7	−128.4	−234.0	+29.2
	2	+125.6			−157.4
	3	−7.1	−95.7	−100.8	−152.4
	4	+79.7	−75.5	−172.1	−185.5
	5		−15.5		
	6		−19.9		
	7		−186.7		
N-III	1	+36.5	−107.3	−139.1	−197.4
	2	+55.2	−106.2	−140.8	−201.3
	3		−108.6	−143.3	
	4		−110.8		
	5	+54.9			−196.4
	6			−146.5	
	9		−106.4		
	10		−111.1		

a) The blank in the table denotes that the site is equivalent to other specific sites. b) Notation of bonds is presented in Figure 1b.

than the other three cases. In the case of N-III, adsorption energies are close to those of pure coronene. For example, adsorption energies at edge sites are +55.2 and +54.9 kJ mol^{-1} for α_2 and α_5 (C–C bond) and +36.5 kJ mol^{-1} for α_1 (C–N bond), whereas +51.3 kJ mol^{-1} for α in pure coronene. Therefore, stability of hydrogen-chemisorbed products is unaffected by edge substitution by nitrogen. Contrary, N-substitution at non-edge sites greatly changes the stabilities of chemisorbed products that depend on the position of nitrogen substitution and hydrogen adsorption.

The results depicted in Table 2 exhibit that the interaction energy between hydrogen and model compounds strongly depends on both the substituted sites of N and adsorbing position of H_2. Nitrogen substitution at inner sites (N-I) gives more stable H-adsorption product, although edge-substitution (N-III) has a small effect. Such wide variety of energy changes is considered to be one reason for the large deviation in experimental results (positive,[18,21,23,24] negative,[25] and no[12] effects), and also suggests the possibility for changing the hydrogen storage properties of carbon materials by nitrogen substitution. Therefore, selective substitutions with nitrogen on graphene-like materials will result in enhancement of their reactivity with hydrogen.

Molecular Orbital Interaction between Hydrogen and Model Molecules. To reveal why the effect of N-substitution varies depending on the positions of nitrogen, we checked the molecular orbital (MO) interaction between hydrogen and model molecules. Here we considered the simplified situation in which the structure of model molecule was fixed. Only the bond length of H–H (d_{H-H}) and the distance between H_2 and model molecule ($R_{coronene-H_2}$) were changed in order to see clearly which MOs of model molecule are important to interact with hydrogen molecule.

Figure 4 shows the two-dimensional potential energy surfaces under the restricted condition stated above. We compared three cases in which H_2 approaches the edge C–C bond at the α site of pure coronene (a), the α_1 site of N-I (b), and the α_3 site of N-II (c). The potential energies were calculated at MP2/6-311G(d,p) level and the structures of model molecules were fixed to their equilibrium structure optimized at HF/6-31G(d,p) level. The saddle point for the H_2 dissociation on pure coronene is at $R_{coronene-H_2} = 1.4$ Å with $d_{H-H} = 1.2$ Å, of which the barrier height is about 550 kJ mol^{-1} from the infinitely separated point. For model N-I, the barrier becomes lower (ca. 420 kJ mol^{-1} at $R_{coronene-H_2} = 1.4$ Å with $d_{H-H} = 1.1$ Å). In the latter case, the slope of the potential energy surface is more gradual than that of pure coronene. On the other hand, in the case of N-II, the activation energy is almost the same as with pure coronene (ca. 530 kJ mol^{-1} at $R_{coronene-H_2} = 1.4$ Å with $d_{H-H} = 1.4$ Å).

Figures 5b, 5d, and 5f show the frontier orbitals of the saddle points shown in Figure 4 and Figures 5a, 5c, and 5e show the corresponding orbitals without H_2. HOMOs of N-I and N-II correspond to LUMO of coronene. In pure coronene, the antibonding orbital of H_2 molecule interacts with the HOMO of coronene that has antibonding character on two edge C–C bonds (77th MO of (a); 77th and 79th MOs of (b)). In the case of N-I, the antibonding orbital of H_2 molecule interacts with the LUMO and HOMO−1 (MOs having antibonding character on α_1 site) of N-I (80th and 78th MOs of (c); 79th and 78th MOs of (d)). Although the LUMO of H_2 is expected to interact with an occupied orbital, the LUMO of N-I interacts with the LUMO of H_2. This would be explained by the small HOMO–LUMO gap of N-I. By interacting with the H_2 molecule, the energy order of the HOMO and LUMO should be easily changed in N-I. The 80th MO (HOMO) of (d) is mainly localized on a bonding orbital (HOMO) of H_2. In the case of N-II, an antibonding orbital of H_2 interacts with the HOMO and HOMO−1 (79th and 78th MOs which have antibonding and bonding (but mainly localized on a_5 carbon atom) character on the α_3 site, respectively, (e)) of N-II (78th and 79th MOs, (f)). Like N-I, the 80th MO (HOMO) of (f) is mainly localized on a bonding orbital of H_2. These results show that nitrogen-substituted molecules have additional occupied orbitals and interact with hydrogen more strongly than pure coronene, decreasing the barrier height of complete dissociation for the chemisorption. In addition, both the HOMO and LUMO of N-I seem to be able to interact with an antibonding orbital of H_2 depending on the hydrogen adsorbing site, since the energy gap between the HOMO and LUMO is small. Therefore, N-I more strongly interacts with H_2 at most hydrogen adsorbing sites than N-II.

Conclusion

Chemisorptions of H_2 on model compounds of N-substituted

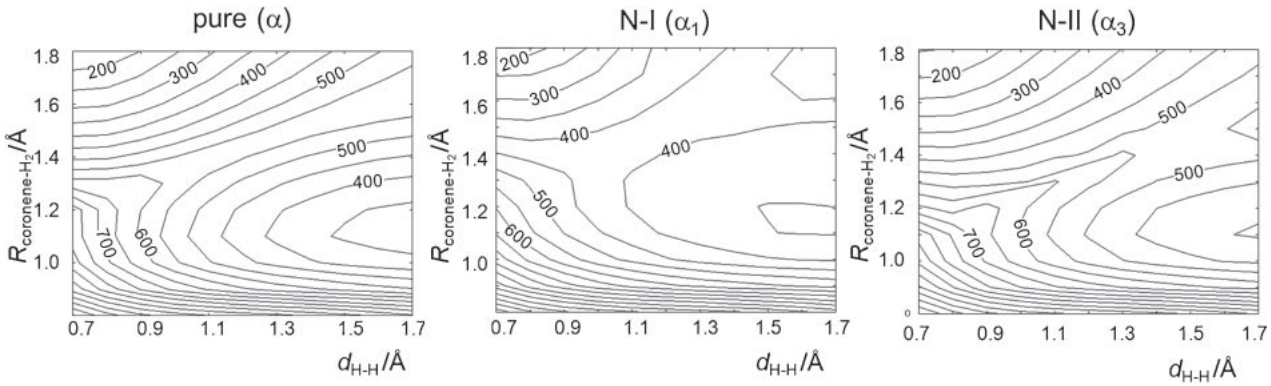

Figure 4. Two-dimensional potential energy surfaces for H_2 approaching an α site of pure coronene (a), α_1 site of model N-I (b), and α_3 site of model N-II (c) (notation of bonds is presented in Figure 1b) as a function of the bond length of H–H (d_{H-H}) and the distance between H_2 and model molecule ($R_{coronene-H_2}$). The distance $R_{coronene-H_2}$ is defined as that between H–H bond and C–C bond to which H_2 approaches in parallel from the top.

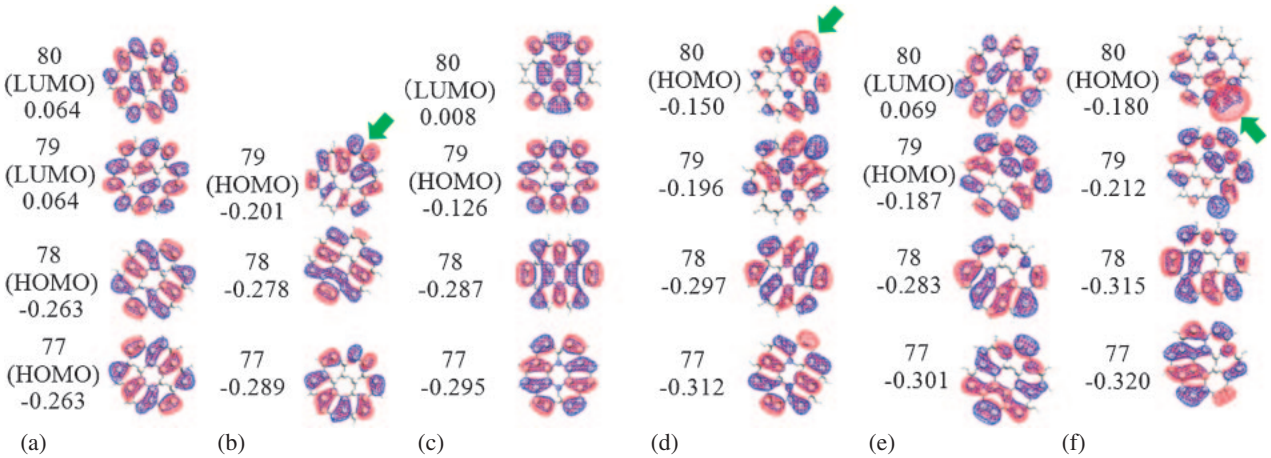

Figure 5. Frontier orbitals of coronene (a), N-I (c), N-II (e), and those of the saddle point structures toward the dissociative H_2 chemisorption onto coronene (b), N-I (d), and N-II (f) shown in Figure 4. The MO numbers and their energies (in hartree) are shown in the left of each orbital. The positions of H_2 molecules are shown by green arrows.

carbon materials were investigated using ab initio molecular orbital calculations. Effects of nitrogen substitution on the interaction energy were discussed for the first time. We assumed coronene as a model structure for fragmented graphene-like material, such as microporous carbon, and examined pure and N-substituted coronenes containing two nitrogen atoms. The stability of the products of H_2 dissociative adsorption is compared in pure and N-substituted cases. Results show that N-substitution at non-edge sites (N-I) stabilizes the chemisorbed products. The results suggest that the interaction energy between hydrogen and carbon materials with a fragmented graphene structure can be practically controlled by N-substitution if the position-selective substitution is experimentally possible. The results might explain the different experimental results of hydrogen storage properties of nitrogen substituted graphene-like materials.

This work has been supported by NEDO (New Energy and Industrial Technology Development Organization) project "Advanced Fundamental Research on Hydrogen Storage Materials (Hydro-Star)." The authors are grateful to Prof. T. Kyotani and Prof. H. Nishihara, Tohoku Univ. for their helpful advice.

References

1 L. Schlapbach, A. Züttel, *Nature* **2001**, *414*, 353.
2 R. Coontz, B. Hanson, *Science* **2004**, *305*, 957.
3 J. Yang, A. Sudik, C. Wolverton, D. J. Siegel, *Chem. Soc. Rev.* **2010**, *39*, 656.
4 A. Züttel, *Naturwissenschaften* **2004**, *91*, 157.
5 L. Zhou, *Renewable Sustainable Energy Rev.* **2005**, *9*, 395.
6 R. C. Lochan, M. Head-Gordon, *Phys. Chem. Chem. Phys.* **2006**, *8*, 1357.
7 S. Orimo, A. Züttel, L. Schlapbach, G. Majer, T. Fukunaga, H. Fujii, *J. Alloys Compd.* **2003**, *356–357*, 716.
8 R. Ströbel, J. Garche, P. T. Moseley, L. Jörissen, G. Wolf, *J. Power Sources* **2006**, *159*, 781.
9 A. Züttel, S. Orimo, *MRS Bull.* **2002**, *27*, 705.
10 A. C. Dillon, M. J. Heben, *Appl. Phys. A: Mater. Sci. Process.* **2001**, *72*, 133.
11 A. Stein, Z. Wang, M. A. Fierke, *Adv. Mater.* **2009**, *21*, 265.
12 H. Nishihara, P.-X. Hou, L.-X. Li, M. Ito, M. Uchiyama, T.

Kaburagi, A. Ikura, J. Katamura, T. Kawarada, K. Mizuuchi, T. Kyotani, *J. Phys. Chem. C* **2009**, *113*, 3189.

13 M. Armandi, B. Bonelli, C. O. Areán, E. Garrone, *Microporous Mesoporous Mater.* **2008**, *112*, 411.

14 L. Chen, R. K. Singh, P. Webley, *Microporous Mesoporous Mater.* **2007**, *102*, 159.

15 R. Gadiou, S.-E. Saadallah, T. Piquero, P. David, J. Parmentier, C. Vix-Guterl, *Microporous Mesoporous Mater.* **2005**, *79*, 121.

16 C. Guan, K. Wang, C. Yang, X. S. Zhao, *Microporous Mesoporous Mater.* **2009**, *118*, 503.

17 H. Nishihara, Q.-H. Yang, P.-X. Hou, M. Unno, S. Yamauchi, R. Saito, J. I. Paredes, A. Martínez-Alonso, J. M. D. Tascón, Y. Sato, M. Terauchi, T. Kyotani, *Carbon* **2009**, *47*, 1220.

18 L. Wang, F. H. Yang, R. T. Yang, *AIChE J.* **2009**, *55*, 1823.

19 T. Ikeda, M. Boero, S.-F. Huang, K. Terakura, M. Oshima, J. Ozaki, *J. Phys. Chem. C* **2008**, *112*, 14706.

20 H. Niwa, K. Horiba, Y. Harada, M. Oshima, T. Ikeda, K. Terakura, J. Ozaki, S. Miyata, *J. Power Sources* **2009**, *187*, 93.

21 B. Viswanathan, M. Sankaran, *Diamond Relat. Mater.* **2009**, *18*, 429.

22 Z. Zhou, X. Gao, J. Yan, D. Song, *Carbon* **2006**, *44*, 939.

23 Z. Yang, Y. Xia, X. Sun, R. Mokaya, *J. Phys. Chem. B* **2006**, *110*, 18424.

24 L. Wang, R. T. Yang, *J. Phys. Chem. C* **2009**, *113*, 21883.

25 X. B. Zhao, B. Xiao, A. J. Fletcher, K. M. Thomas, *J. Phys. Chem. B* **2005**, *109*, 8880.

26 C. Liu, Y. Y. Fan, M. Liu, H. T. Cong, H. M. Cheng, S. Dresselhaus, *Science* **1999**, *286*, 1127.

27 T. Fukunaga, K. Itoh, S. Orimo, M. Aoki, H. Fujii, *J. Alloys Compd.* **2001**, *327*, 224.

28 Y. Miura, H. Kasai, W. Diño, H. Nakanishi, T. Sugimoto, *J. Appl. Phys.* **2003**, *93*, 3395.

29 J. O. Sofo, A. S. Chaudhari, G. D. Barber, *Phys. Rev. B* **2007**, *75*, 153401.

30 D. C. Elias, R. R. Nair, T. M. G. Mohiuddin, S. V. Morozov, P. Blake, M. P. Halsall, A. C. Ferrari, D. W. Boukhvalov, M. I. Katsnelson, A. K. Geim, K. S. Novoselov, *Science* **2009**, *323*, 610.

31 Y. Li, R. T. Yang, *J. Phys. Chem. C* **2007**, *111*, 11086.

32 M. Kayanuma, U. Nagashima, H. Nishihara, T. Kyotani, H. Ogawa, *Chem. Phys. Lett.* **2010**, *495*, 251.

33 G. M. Psofogiannakis, G. E. Froudakis, *J. Phys. Chem. C* **2009**, *113*, 14908.

34 G. M. Psofogiannakis, G. E. Froudakis, *J. Am. Chem. Soc.* **2009**, *131*, 15133.

35 Z. H. Zhu, G. Q. Lu, H. Hatori, *J. Phys. Chem. B* **2006**, *110*, 1249.

36 M. W. Schmidt, K. K. Baldridge, J. A. Boatz, S. T. Elbert, M. S. Gordon, J. H. Jensen, S. Koseki, N. Matsunaga, K. A. Nguyen, S. Su, T. L. Windus, M. Dupuis, J. Montgomery, Jr., *J. Comput. Chem.* **1993**, *14*, 1347.